7. LOCAL AERATION CHARACTERISTICS
(Kobus, Renner)

7.1 General Remarks

Free-surface flow conditions generating air-water mixtures can be categorized broadly into flow configurations causing ambient surface aeration - such as high-speed open channel flows or jets, which have been treated in the previous chapters - and those giving rise to local aeration. The basic difference between the two types of flow is the fact that in local aeration processes the transport capacity of the flow may drastically differ from its local entrainment capacity, whereas these capacities are always balanced in fully developed flows of ambient surface aeration. In high speed open channel flow, for instance, air is entrained at the highly turbulent free surface all along the channel up to the point where the transport capacity of the flow is reached and equilibrium conditions prevail. In local surface aeration, air may be entrained due to a local disturbance of the free surface at a rate completely independent of the transport capacity: the latter is only of importance with regard to the question how far and for how long the air is kept in suspension. It depends upon the transport capacity of the flow, therefore, whether the entrained air is transported with the flow or rather quickly discharged into the atmosphere again, thus rendering the process of self aeration as of local importance only.

A typical case of local air entrainment is the classical hydraulic jump, which entrains a considerable amount of air locally at the toe of the surface roller, but because of little or no air transport capacity, discharges most of it back into the atmosphere through the roller surface, so that after a short distance downstream the air content of the flow is almost zero again. This configuration will be treated in chapter 7.2, since knowledge of the entrainment rate is of importance for evaluating the effectiveness of a hydraulic jump as an in-stream aeration device for water quality improvement. A closely related phenomenon is the hydraulic jump forming in a closed conduit leading from free-surface to pressure flow, where the entrained air is trapped and may affect the downstream flow conditions seriously, as is evidenced from the literature on two-phase pipe flows [116, 85] . The trapped air may collect in large pockets and give rise to flow instabilities ("blowout" or "blowback") which may cause dangerous vibrations and structural damage.

Local self-aeration occurs also whenever a liquid jet impinges upon a solid surface (e.g. in the deflection of a free jet in a closed dissipation chamber, or in the process of priming a siphon) or penetrates a liquid surface at a substantial velocity difference (e.g. in drop structures, in wastewater outfalls located above the free surface, or downstream of sharp-crested weirs). Air may also be entrained locally by vortices or by breaking waves. In all these cases, the flow conditions give rise to self-aeration processes which will be treated in chapters 7.3. to 7.5.

In order to define the scope of this chapter, it is important to distinguish these cases of "self-aeration" from "forced"-surface aeration processes, which will not be considered here. We term "forced" aeration all those cases in which a flow is generated specifically for the purpose of air entrainment. This includes e.g. water jet pumps or all devices which artificially disturb the surface by propellers, rotors or pumps etc. in order to generate an air-water mixture, as they are commonly applied in wastewater treatment.

Renner [142] has done a comprehensive literature study of flow configurations causing local self-aeration and compiled the data given in Figs. 7.1 and 7.2 for two-dimensional and axisymmetric flow configurations, respectively. In these graphs, the relative air discharge is plotted as a function of the Froude number for various boundary geometries. Although not all data published in the literature should be taken at face value, these diagrams give a general idea of the relations and order of magnitude involved. They also show, that a unified treatment of all cases of local self-aeration is not possible, but that the peculiarities of each flow configuration have to be studied carefully and separately. This will be done in the following sections for the basic configurations of the hydraulic jump, a two-dimensional jet impinging on a solid surface, and a round jet penetrating a liquid surface. Although generally the more complicated geometries are technically more important, this treatise is restricted to the simpler cases mentioned above in order to gain a physical and quantitative understanding of the processes involved and some insight into the mechanisms of self-aeration. It is hoped that this may provide a sound basis for further research tackling the more complex configurations and lead to a more rational approach to such technical problems as air demand of regulating devices and high-head installations etc.

Most cases of local aeration have in common that the air entrainment takes place at a discontinuity of the free surface at which substantial velocity differences are encountered. In a hydraulic jump, for instance, the air is entrained exclusively at the toe of the surface roller. The same is seen to be true for jets impinging on solid surfaces, and in jets penetrating into a stagnant body of liquid, air is entrained along the circumference of the jet intersecting the free surface of the liquid. In all these instances, the process of air entrainment can be visualized as air pockets being trapped between roller (or liquid surface) and inflow and then being carried away in the downstream direction. The size and frequency of formation of such pockets can reasonably be expected to depend upon the differential velocity between roller and inflow, or - since the former is zero in the mean - upon the velocity of the inflow alone. Obviously, the boundary scale - for instance, the water depth or jet width t_o - will in most cases have no influence upon the entrainment process unless the water depth becomes small enough to be of the order of the enclosed air pockets.

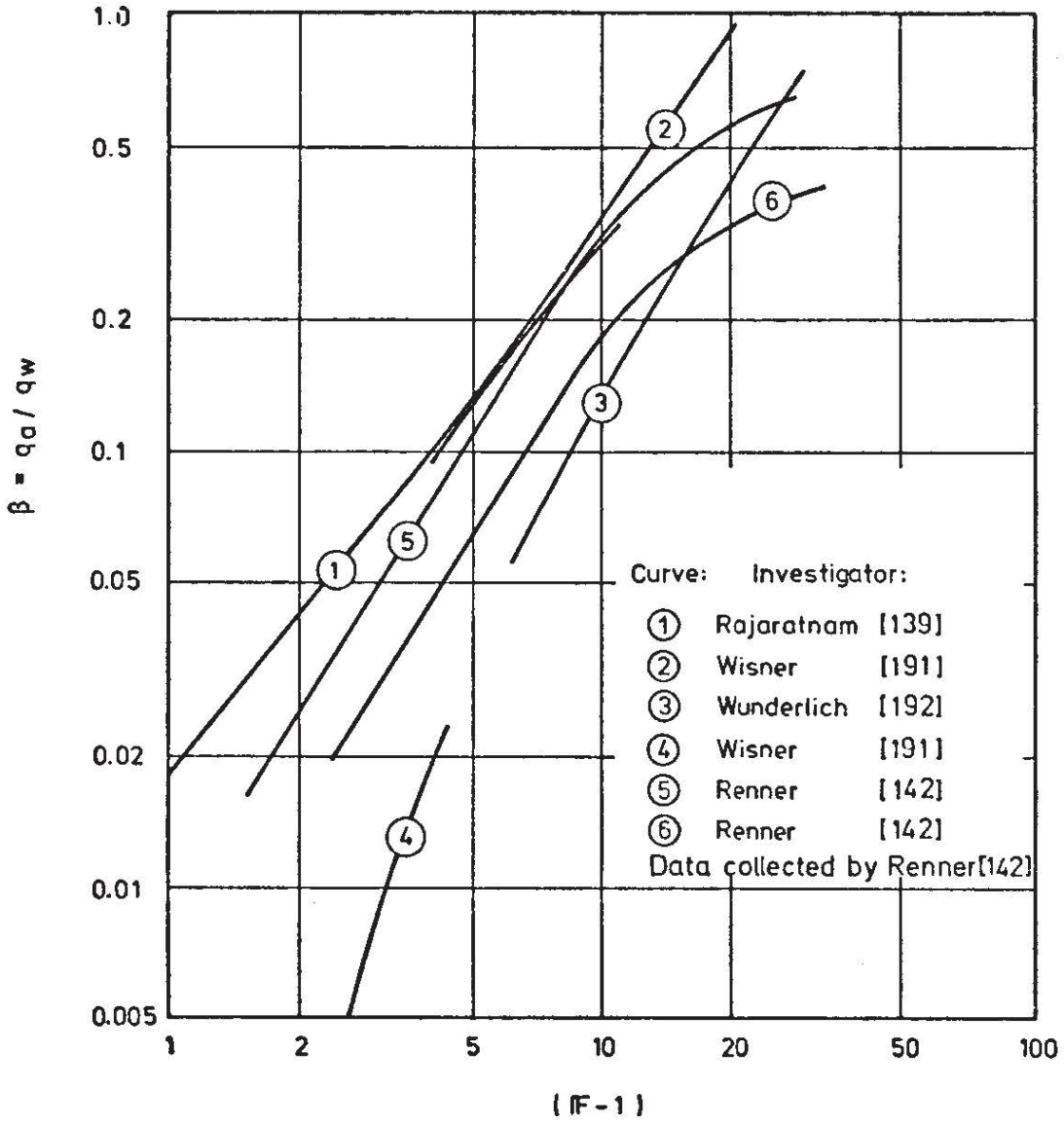

Flow configurations :

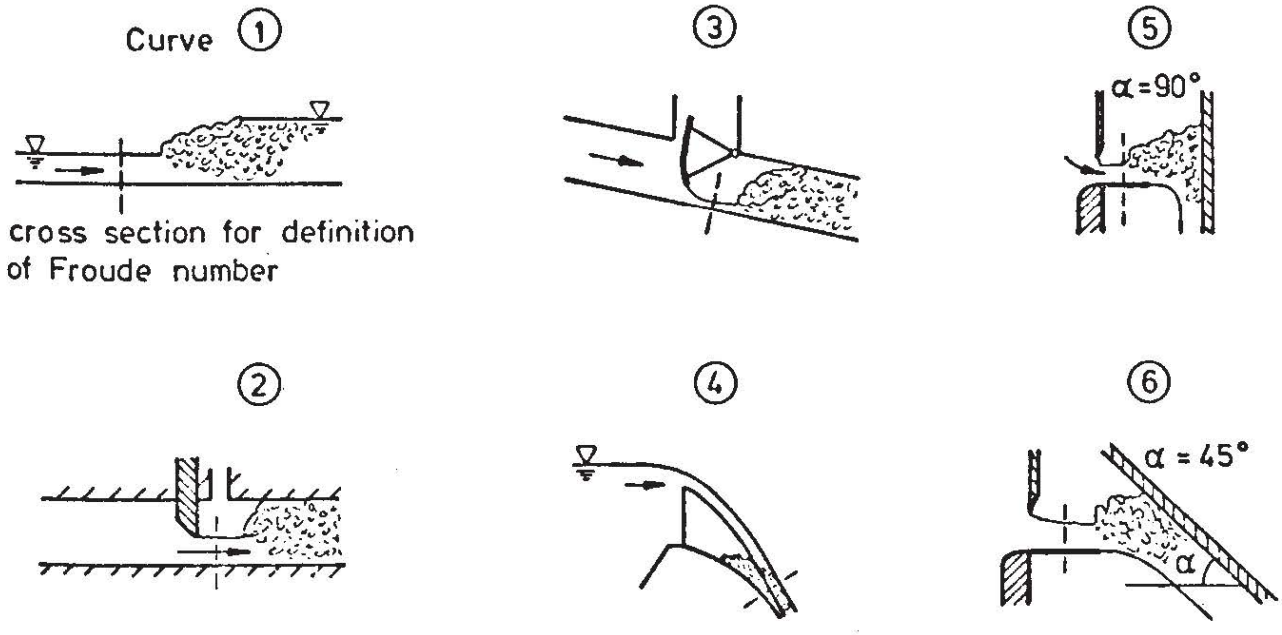

FIG. 7.1 RELATIVE AIR ENTRAINMENT FOR VARIOUS TWO-DIMENSIONAL FLOW CONFIGURATIONS ACCORDING TO RENNER [142]

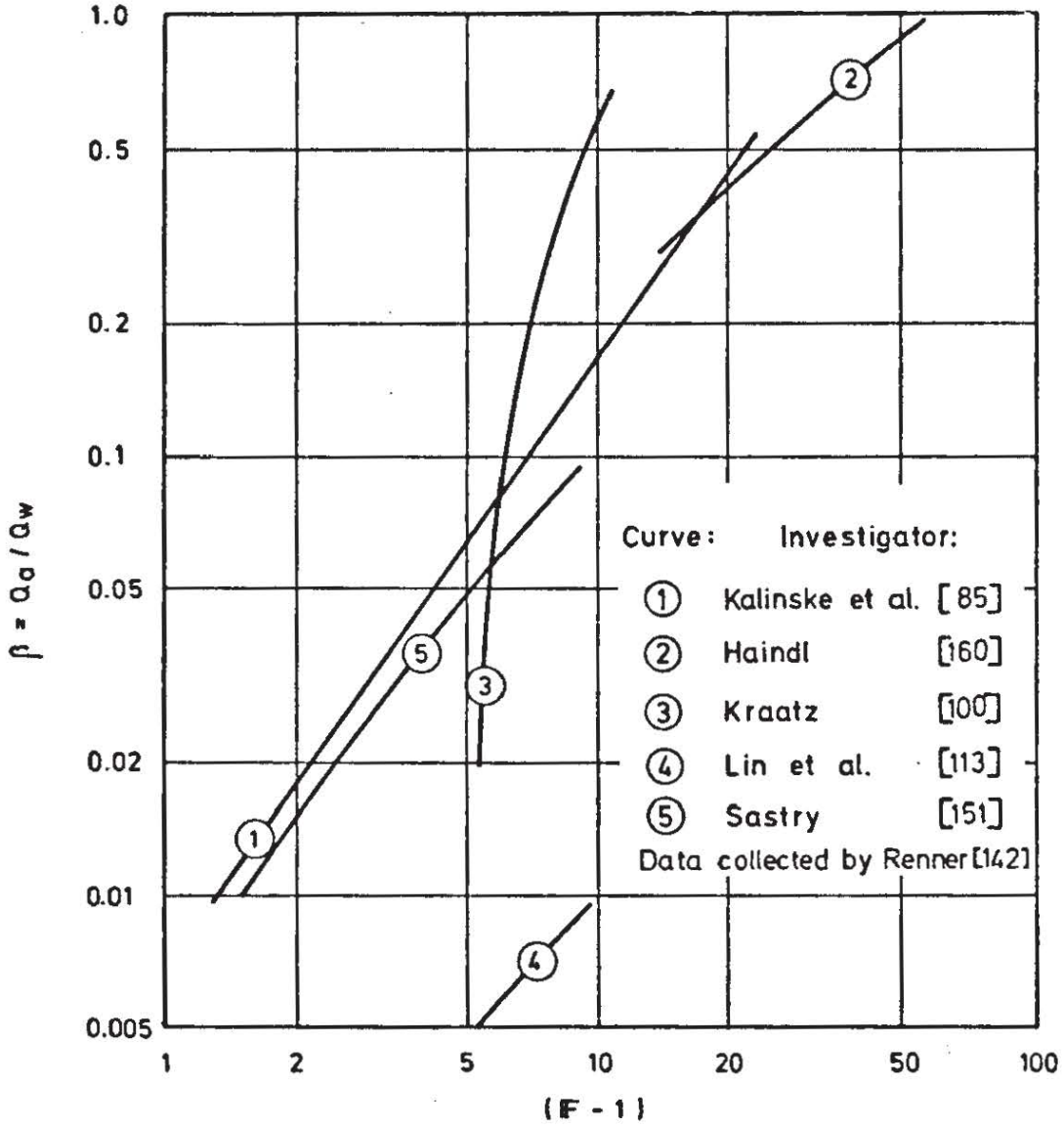

Flow configurations:

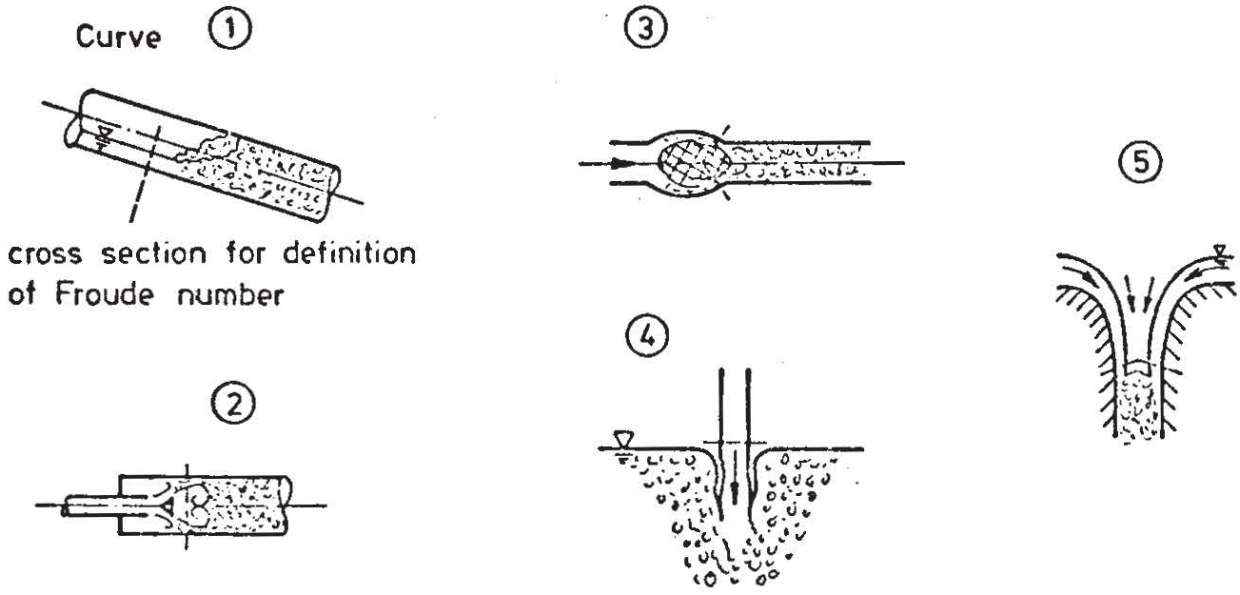

FIG. 7.2 RELATIVE AIR ENTRAINMENT FOR VARIOUS AXISYMMETRICAL FLOW CONFIGURATIONS [142]

For air entrainment processes which are not affected by the boundary scale, it has been shown in chapter 3 that under fully turbulent conditions one obtains from the functional relationship

$$q_{a,e} = f(v_o ; \rho_w ; g) \tag{7.1}$$

by dimensional analysis

$$\frac{q_{a,e}}{v_o^3 / g} = \text{const} \equiv k_e \tag{7.2}$$

The same result is obtained for axisymmetric conditions, if q_{ae} is interpreted as the air entrained per unit length of the circumference. Relationship (7.2) can be transformed to yield an expression for the relative air entrainment β_e as a function of the Froude number:

$$\frac{q_{a,e}}{q_w} = k_e \frac{v_o^3 / g}{v_o t_o} = k_e \frac{v_o^2}{g t_o} \quad ; \qquad \beta_e = k_e \cdot F^2 \tag{7.3}$$

It is important at this point to distinguish clearly between air entrainment and air transport. The local air entrainment rate β_e is given by the ratio of the amount of air per unit time actually entrained into the flow to the water discharge, whereas the relative air discharge β relates the air transported out of the downstream control section to the water discharge. Thus the local value of β in a hydraulic jump varies from the maximum value of β_e near the toe to zero at the downstream end of the jump, because the flow has no transport capacity and hence all the air is lost to the atmosphere. On the other hand, if all the entrained air would be trapped and carried away by the flow, then β would be constant and equal to β_e all along the channel.

For any given problem of local self-aeration, either the local air entrainment rate β_e or the downstream transport capacity of the flow may provide the limiting condition for the process. The limit provided by the local air entrainment capacity is given by eq. 7.3. However, deviations from this relation are to be expected whenever the transport capacity of the flow provides the limiting condition. For any flow configuration, there exists a certain saturation concentration and hence a maximum transport capacity which cannot be superseded. According to Brauer [15] , tests with air bubbles in water columns yielded a maximum possible air concentration of about 40 %, in which case there was still considerable "mobility" of the individual bubbles. For a suspension of uniform spheres, a dense packing without any mobility of the individual spheres would correspond to a concentration of 60%. The maximum value which can actually be attained

in an air-water mixture depends upon the size composition of the bubble mixture, but it seems reasonable to assume the maximum possible concentration to be about 40 to 50%. The mean volume concentration $\bar{C}$ is defined as

$$\bar{C} \equiv \frac{\forall_a}{\forall_a + \forall_w} \tag{7.4}$$

For conditions of zero or negligible slip velocity between air and water, this is related to the relative air discharge by

$$\beta \equiv \frac{Q_a}{Q_w} = \frac{\bar{C}}{1-\bar{C}} \quad (\text{for } u_a = u_w) \tag{7.5}$$

Hence a saturation concentration of 40 to 50% corresponds to an upper limit for β of

$$\beta \leq \beta_{sat} \approx 0.67 \text{ to } 1.0 \tag{7.6}$$

According to the foregoing considerations, one can state now several limiting conditions for local self-aeration processes in free surface flows, namely an "inception limit", an "entrainment limit" and a "transport limit".

Inception limit: The flow conditions must be such as to generate a sufficiently large disturbance for air entrainment to occur. The inception limit depends strongly upon the particular flow configuration, and hence no general relation specifying this limit can be given. In a hydraulic jump, the inception limit is obviously given by ($\mathbb{F} > 1$); and in general a certain minimum Froude number must be exceeded, the value of which depends upon the particular boundary geometry (e.g. the jets treated in chapter 7.3 must strike the wall in order to cause air entrainment, etc.).

Entrainment limit: Whenever the entrainment capacity provides the limiting condition, the relative air discharge is described by a relation of the type

$$\beta = k\, \mathbb{F}^2$$

where k is constant as long as the entrainment process is not affected by the local boundary scale.

Transport limit: The transport capacity of the flow is limited absolutely by the maximum air concentration possible, which restricts the relative air discharge to values of

$$\beta \leq \beta_{sat} \approx 0.67 \text{ to } 1.0$$

The air-transport capacity may be limited further by the downstream flow conditions, depending upon the particular boundary geometry and the hydodynamic parameters characterizing the relative importance of various fluid

properties. These conditions, again, cannot be specified generally.

7.2 Air Entrainment in a Hydraulic Jump

The aeration characteristics of a free hydraulic jump have been studied experimentally by various investigators, in particular by Rajaratnam 1962 [139] , Schröder 1963 [155] , and more recently by Resch and Leutheusser [145, 109] . All these investigations confirm Rajaratnam's observation that the mean air concentration $\bar{C}$ (averaged over a vertical cross section) attains its maximum value $\bar{C}_{max}$ within a very short distance from the toe of the jump, and that, after this almost instantaneous increase, the mean air concentration drops steadily in the downstream direction. A substantial part of the entrained air is lost through the surface of the roller, and eventually all air escapes again into the atmosphere (Figs. 7.3 and 7.5). This indicates that air entrainment into the water flow takes place only at the toe of the surface roller (an observation which is also supported by the fact that in submerged jumps, which have no toe, no air entrainment takes place), and that a determination of the total amount of air entrained has to be based on the maximum air concentration observed near the toe. To be sure, there is considerable exchange of air through the roller surface in both directions, but according to the mean concentration profiles there is always a net transport of air out of the water.

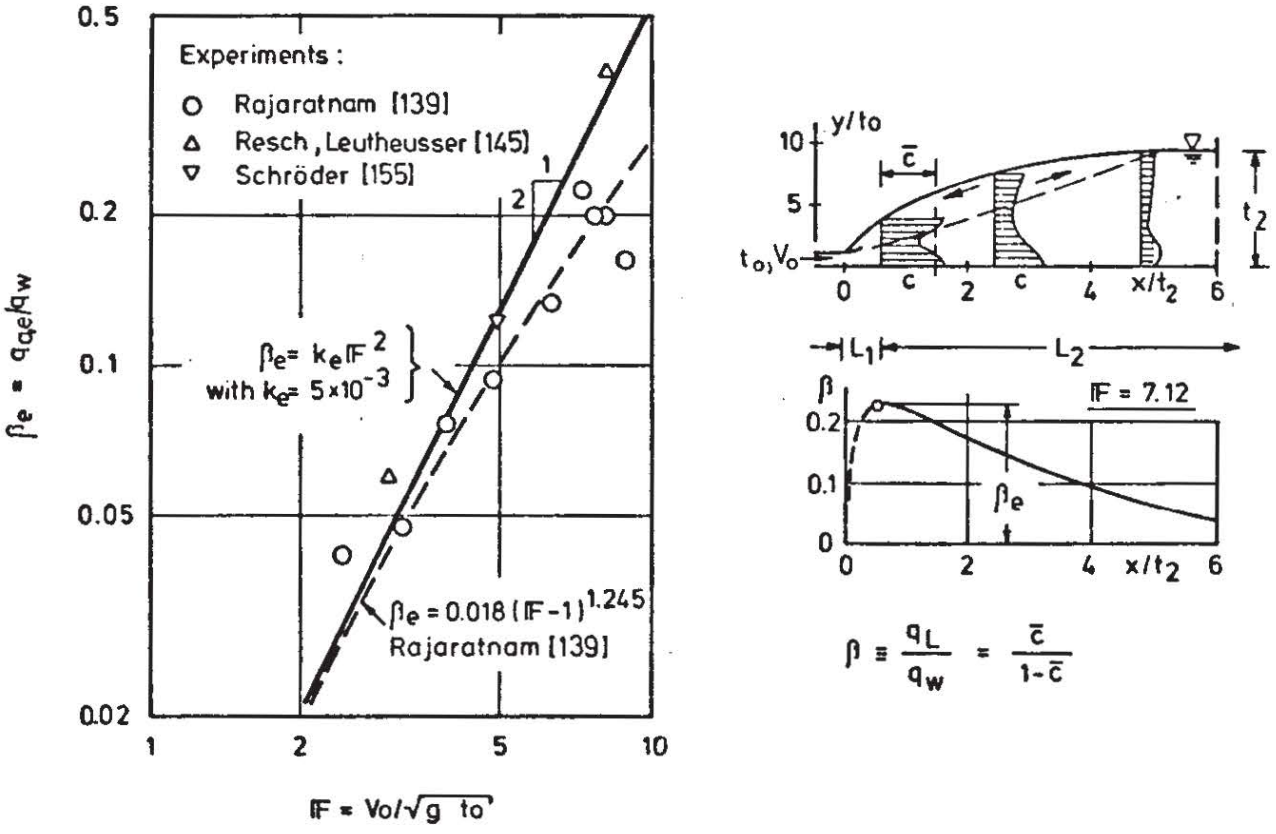

FIG. 7.3 AIR ENTRAINMENT IN A HYDRAULIC JUMP

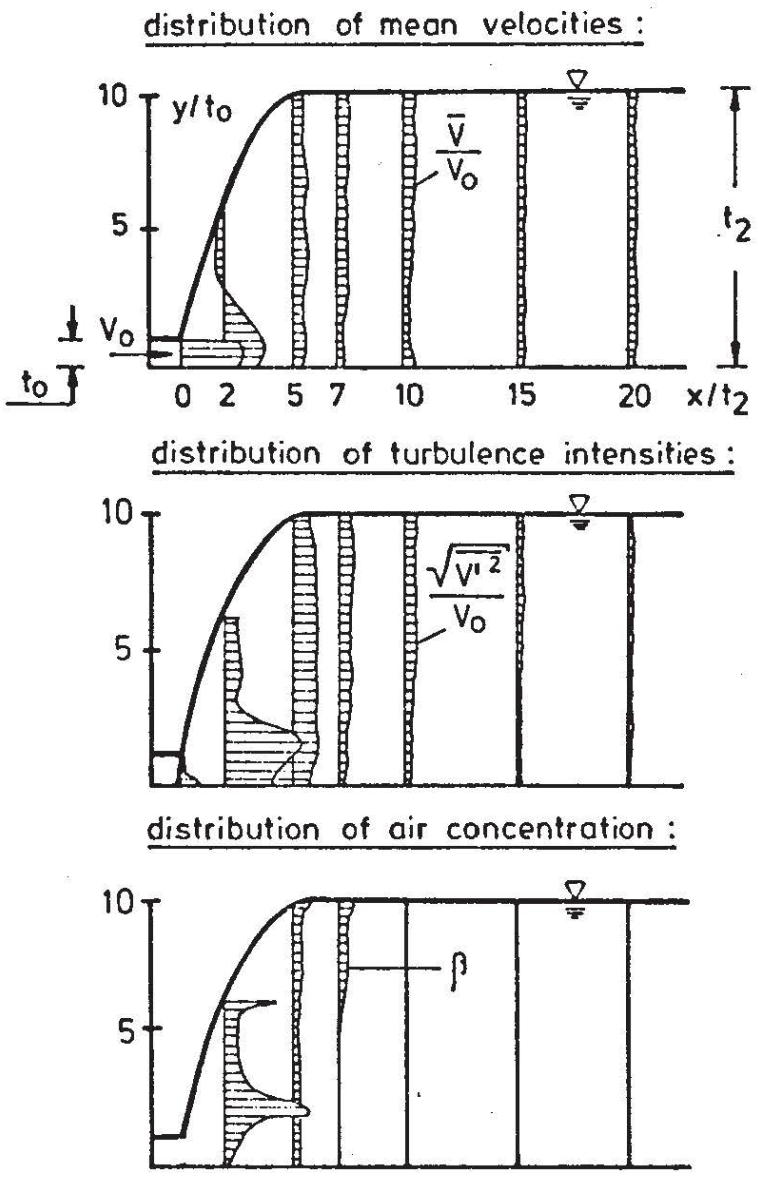

FIG. 7.4 VELOCITY AND CONCENTRATION DISTRIBUTION IN A HYDRAULIC JUMP [145]

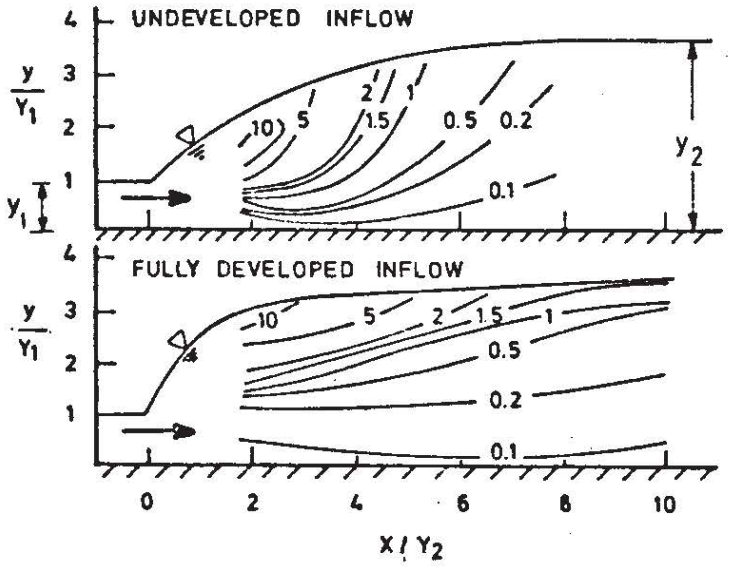

FIG. 7.5 DISTRIBUTION OF VOID RATIO IN JUMPS OF $F_1 = 2.85$ ACCORDING TO LEUTHEUSSER [109]

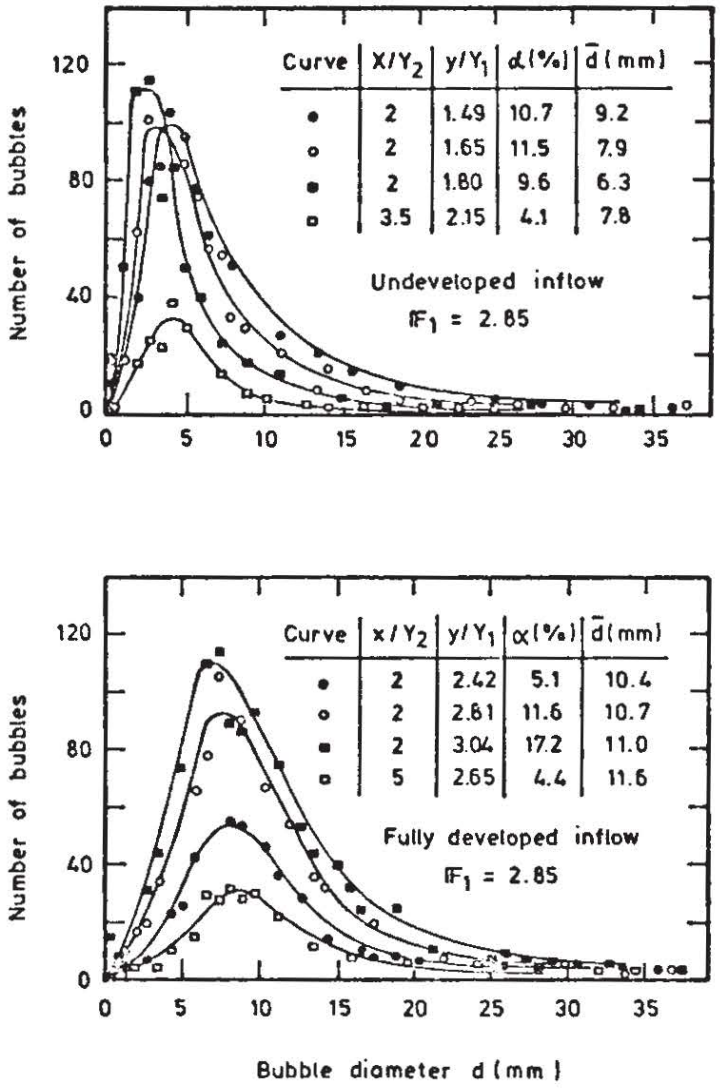

FIG. 7.6 STATISTICAL DISTRIBUTION OF BUBBLE SIZES FOR JUMPS OF $F = 2.85$ [109]

The ratio of the amount of air entrained per unit time to the water discharge, or the relative air entrainment β_e, is given according to Rajaratnam by

$$\beta_e = \frac{q_{a.e}}{q_w} = 0.018\,(F-1)^{1.245} \quad \text{with} \quad F \equiv \frac{V_o}{\sqrt{g\,t_o}} \qquad (7.7)$$

This relation was developed with the aid of eq. 7.5, which holds true only if there is no slip between air and water - a justified assumption in view of the fact that the water velocities at the toe of the jump are large and the mean bubble sizes generated seem to be rather small (Fig. 7.6). Resch and Leutheusser [145] measured both turbulence and concentration distribution in a hydraulic jump by means of a hot film technique. From their concentration profiles, Renner [142] evaluated the relative entrainment β_e, which is plotted, together with Rajaratnam's results, in Fig. 7.3. This figure also contains data obtained from Schröder's [155] experiments. A comparison of the results shows that both Resch and Leutheussers's and Schröder's data show higher values of β_e at comparable Froude numbers than Rajaratnam's results.

The deviations may be due to experimental uncertainties, since each investigator used a different technique of measurement, none of which has been proven to be beyond any doubt (Rajaratnam used conductivity probes, Schröder optical counts of the bubbles, Resch and Leutheusser used hot film probes). Furthermore, Resch and Leutheusser's investigations have shown that the shape of the velocity profile at the inflow has a pronounced influence upon turbulence and concentration distributions within the jump (Fig. 7.5). These conditions may have varied in previous investigations and thus have given rise to scatter of the data.

Fig. 7.3 also contains a straight line representing a functional relation between β_e and F of the form given by eq. 7.3. Considering the scatter inherent in the available experimental data, the observations of all investigators seem to bear out such a relationship fairly well, with the proportionality factor k_e having a magnitude of

$$k_e = 5 \times 10^{-3} \quad (\pm 20\%) \tag{7.8}$$

for the free hydraulic jump. It is assumed that this relationship holds true for air entrainment due to a surface roller in general. In other flow configurations (like a jet striking a wall, for instance) it would then depend upon the particular boundary geometry and the downstream transport capacity, which portion of the entrained air is actually carried away, and how much air escapes again through the roller surface. For all cases of local air entrainment through a surface roller, the value of k_e given by eq. 7.8 can therefore be considered as a maximum which cannot be exceeded ($k \leq k_e$).

Whereas air entrainment due to a hydraulic jump in an open channel usually offers no engineering problems (apart from the beneficial contribution of oxygen recharge), its counterpart in a pipe leading from free-surface flow to flow under pressure can pose severe problems: the air entrained by the jump is initially transported downstream by the flow and, depending upon the geometrical and flow conditions, may collect to form large bubbles which may eventually "blow out" in the downstream direction or "blow back" upstream. Such unsteady flow conditions may result in high forces not accounted for in the design and hence may lead to structural damage [116] . It is therefore important to know how large the air entrainment will be for this flow configuration.

Kalinske and Robertson [85] have studied the air entrainment due to a hydraulic jump in a circular pipe. A dimensional analysis of the parameters involved yields

$$\beta \equiv \frac{Q_a}{Q_w} = f \left(F_1 ; S ; t_1 / D \right)$$

where the Froude number is formed using the upstream velocity and the fictitious depth given by the crossectional area divided by the surface width, and S is the slope of the pipe. Their experiments showed, that for slopes

from 0 to 30 % and relative upstream water depths t_1/D from 0.1 to 0,6, the relative air entrainment proved to be independent of S and t_1/D and to be a unique function of the Froude number, represented by an equation of the form

$$\beta = 0.0066 \ (F-1)^{1.4} \qquad (7.9)$$

The corresponding two-dimensional case of air entrainment behind a high-head gate in a rectangular duct has been investigated by Wisner [191] . From prototype measurements, he derived as an upper limit of air entrainment for that configuration the relation

$$\beta \leq 0.014 \ (F-1)^{1.4} \qquad (7.10)$$

In comparing the ß-values according to eqs. 7.9 and 7.10 to those for $ß_e$ in a free hydraulic jump given by eqs. 7.3 and 7.8, it is seen that, for the Froude number range investigated (and practically feasible), the values $ß_e$ for the free jump are always larger than the relative air discharge ß

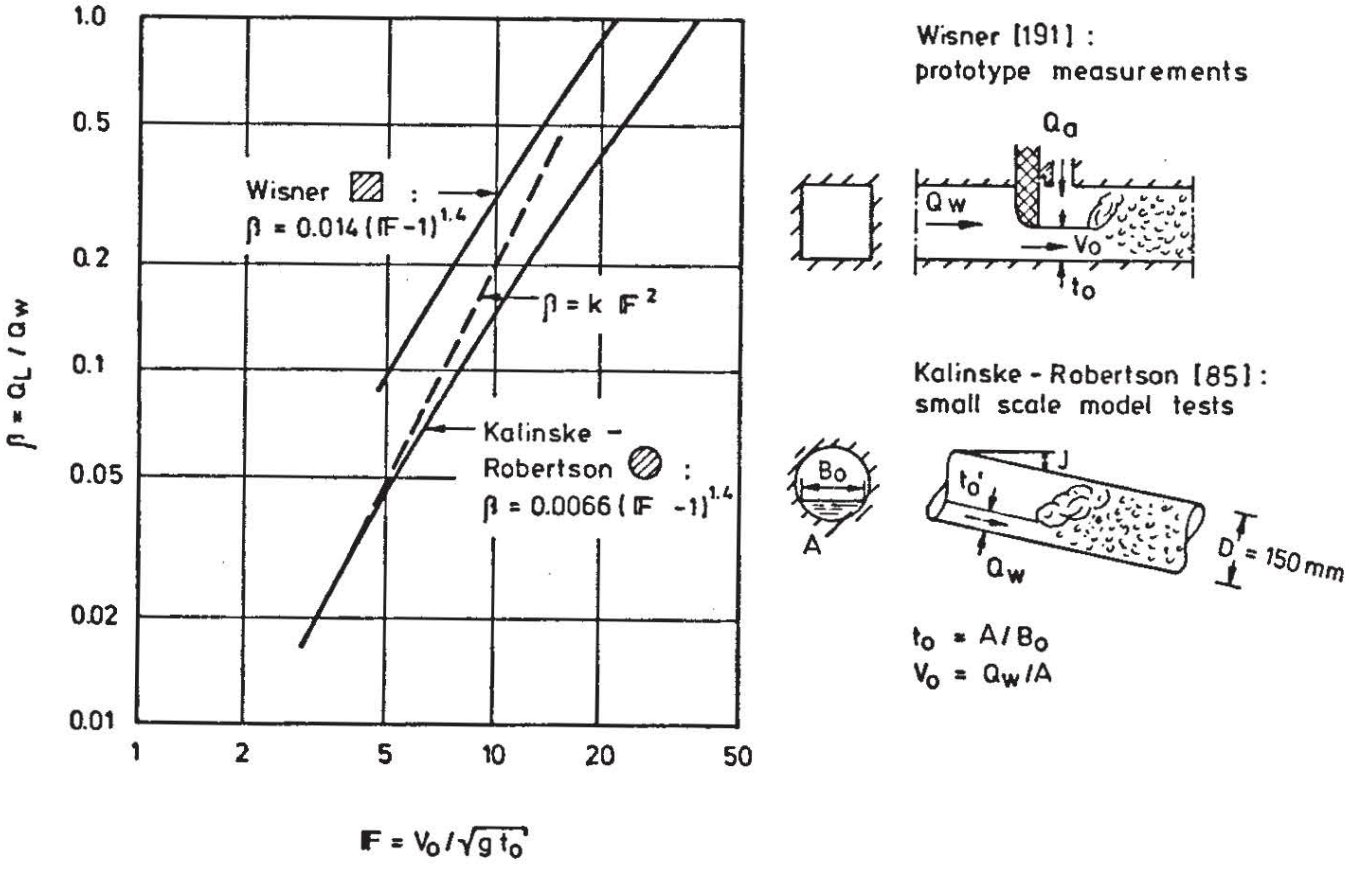

FIG. 7.7 AIR ENTRAINMENT IN A HYDRAULIC JUMP IN CLOSED CONDUITS

carried downstream by the pipe flow. This is reasonable in view of the observation that some of the air entrained at the toe will escape through the surface roller again, so that not all entrained air will still be trapped in the water at the point where the conduit begins to flow full, and hence the downstream air discharge (which was measured) must be smaller than the total air entrainment rate.

There are a number of further experimental investigations for particular boundary conditions. Wunderlich [192] studied the air demand behind vertical plane and sector high-head gates; Wisner [191] investigated the air entrainment of a hollow jet valve, and Kraatz [100] determined the air demand of a ring-piston valve. The results of these studies are also presented in terms of β versus $\mathbb{F}$ diagrams, in Figs. 7.1 and 7.2.

7.3 Air Entrainment of a Jet Impinging on a Rigid Surface

When a (non-vertical) free water jet impinges on a (non-horizontal) plane rigid surface, the jet is deflected downward, while at the top side a surface roller is formed, which interacts with the jet flow. Such a surface roller causes local aeration, much like in a hydraulic jump, by trapping air at the toe of the roller and transporting it downstream. Apart from this interaction of a high velocity free-surface flow with a surface roller consisting of an air-water mixture, the two flow situations differ considerably, however, insofar as in a hydraulic jump a considerable deceleration of the flow is caused by the pressure force on the downstream side, whereas jet impingement upon a rigid surface primarily causes a deflection of the jet in a different direction without changing the magnitude of the velocity considerably. The surface roller (in both cases) actually is a zone of flow separation, which interacts and exchanges fluid with the mean flow due to the intensive shear at the separating streamline.
Renner [142] has investigated the air entrainment due to a two-dimensional jet impinging on a vertical or inclined wall as shown in Figs. 7.8 and 7.9. With reference to the definitions given there, the following set of parameters has to be considered in treating the problem:

$$\frac{Q_a}{B} = q_a = f\,(V_o; t_o; L; a; \alpha; \theta_o; \Delta p; \rho_w; g; \mu_w; \sigma) \qquad (7.11)$$

This can be reduced by dimensional analysis to the following relationship:

$$\frac{q_a}{v_o t_o} = f\left(\frac{L}{t_o}; \frac{a}{t_o}; \alpha; \theta; \frac{\Delta p}{\rho_w V_o^2}; \frac{V_o}{\sqrt{g t_o}}; \frac{V_o t_o}{\mu_w/\rho_w}; \frac{V_o}{\sqrt{\sigma/\rho_w t_o}}\right) \qquad (7.12)$$

or (by definitions)

$$\beta = f\left(\frac{L}{t_o}; \frac{a}{t_o}; \alpha; \theta_o; \frac{\Delta p}{\rho_w V_o^2}; \mathbb{F}; \mathbb{R}; \mathbb{W}\right)$$

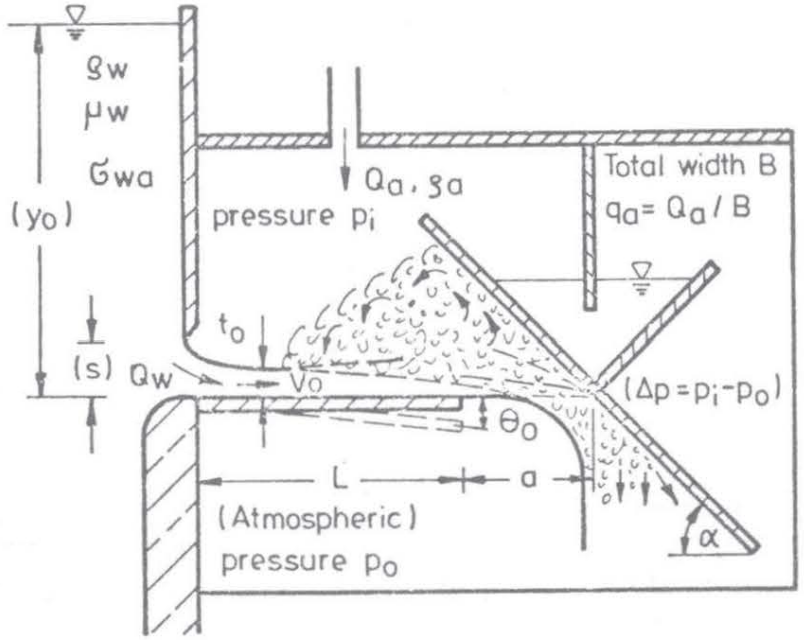

FIG. 7.8 DEFINITION SKETCH FOR RENNER'S INVESTIGATION OF A TWO-DIMENSIONAL JET IMPINGING ON A RIGID SURFACE [142]

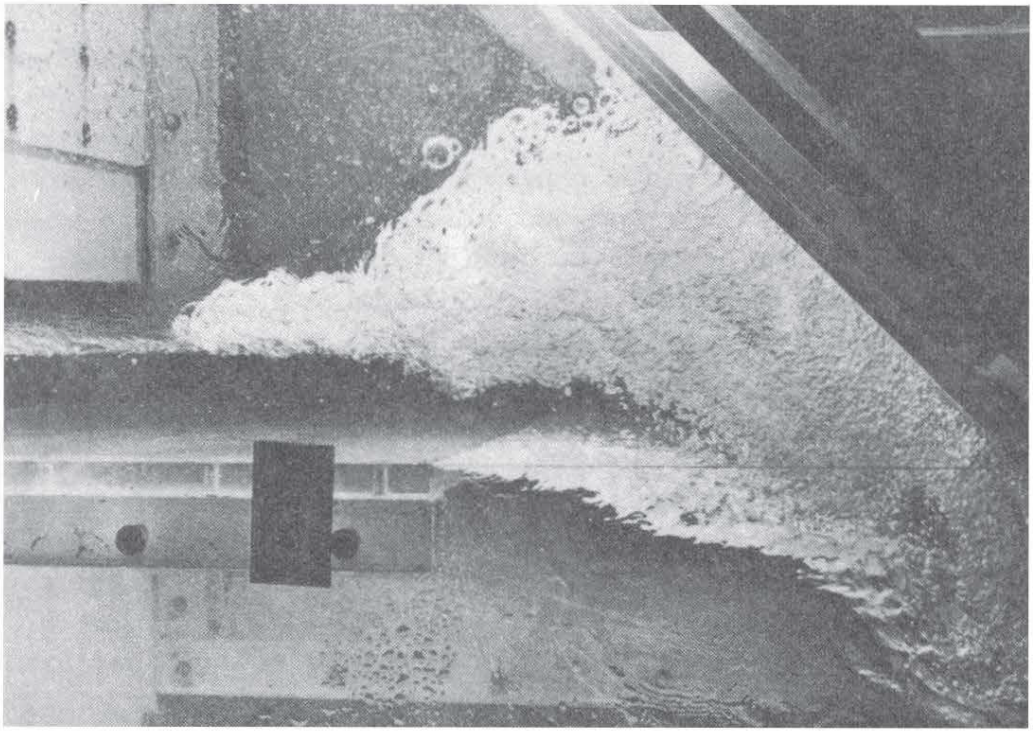

FIG. 7.9 AIR ENTRAINMENT IN A JET STRIKING A RIGID SURFACE

In order to treat this relationship experimentally, the following restrictions and simplifications were introduced and checked experimentally:

- the study is restricted to $\Delta p/(\rho_w v_o^2)=0$, i.e. the pressure on both sides of the jet is atmospheric, $(p_i = p_o)$.

- the length L of the leading plate is always kept small enough so that the turbulent boundary layer of the plate is very much smaller than the water depth t_o. In this case, the parameter L/t_o can have no influence upon the air entrainment. In the experiments, L/t_o varied from 0 to 120 without affecting the results.

- for fully turbulent flows, neither the Reynolds number nor the Weber number have any bearing upon the air entrainment, since the inertial reactions and gravitational forces dominate the process and are very much larger than forces due to viscosity or surface tension. In the experiments, the Reynolds numbers ranged from 1×10^4 to 5×10^5, and Weber numbers from 40 to 200. Within these limits, no influence of either one upon the processes studied was found.

- the underlying assumption of two-dimensionality was verified by test runs, in which the relative jet width B/t_o was varied from 8 to 200 without having a noticeable effect upon the results.

With these assumptions, the relation 7.12 reduces to

$$\beta = f\left(\mathbb{F}\,;\,\frac{a}{t_o}\,;\,\alpha\,;\theta_o\,;\,\frac{L}{t_o}\right) \qquad (7.13)$$

i.e. the relative air entrainment ß is a function of the Froude number and the local boundary geometry.

Renner conducted extensive experiments to investigate relation 7.13 experimentally. He used jets with and without leading plate and varied both the distance a and the angle of inclination α of the impingement plate over a wide range. He studied mainly horizontal jets ($\theta_o = 0$), but also obtained some results for $\theta_o = 5°$ and $10°$ sloping downward.

The air which is trapped at the toe of the surface roller is transported in the downstream direction and, due to intensive shear action, is spread both upward and downward from the dividing streamline at an unknown rate (Fig. 7.10). The distribution of air bubbles over the cross section is a result of the combined action of the air bubbles' buoyancy, tending to cause a net upward transport, and the turbulent velocity fluctuations in combination with a positive concentration gradient in the upward direction. Interaction of both effects leads to the development of a time-averaged concentration distribution, much similar to its (upside down) counterpart of suspended sediment transport in an open channel flow.

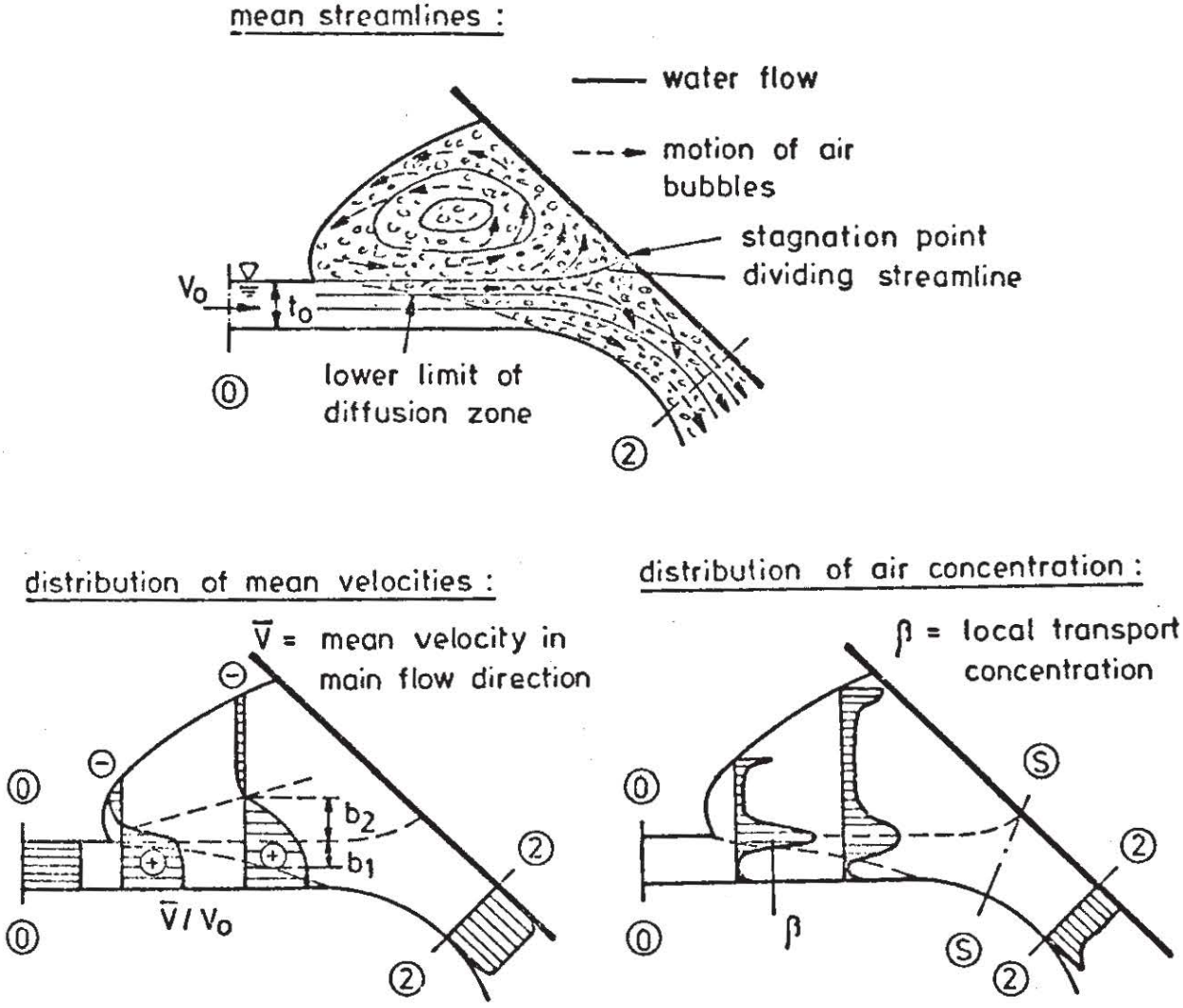

FIG. 7.10 QUALITATIVE VELOCITY AND CONCENTRATION DISTRIBUTION FOR A JET IMPINGING ON AN INCLINED WALL

When the jet hits the wall, the air bubbles contained above the dividing streamline are deflected upward and are either recirculated or emerge through the roller surface, thus not contributing to the net transport of air out of the upper chamber, whereas the air bubbles contained below the dividing streamline are deflected downward and out of the control region: this part constitutes the air discharge which is actually measured.

It is important to note that the air bubbles react differently to the pressure field in the region of jet deflection than the surrounding water because of their extremely small inertia; they tend to follow a pressure gradient more readily. This effect tends to offset any deviations between air bubbles and water particles due to the bubble slip velocity, which one might expect to be significant predominantly in the stagnation region, where the water velocities are small.

Since the water velocities at cross section S (Fig. 7.10) are usually much larger than the rising velocity of the air bubbles contained in the flow, it can safely be assumed that all the air transported through section S will be transported out of the control volume and hence constitutes the amount of air removed from the upper chamber per unit time. This quantity, to be sure, is always smaller than the entrainment rate β_e at the toe of the roller, since a considerable amount of air is spreading above the dividing streamline. The amount of air bubbles rising through the dividing streamline due to buoyancy must increase with decreasing turbulence intensity: although this may not be significant in the present case, it is seen to be predominant in a free hydraulic jump (where air transport eventually becomes zero).

From this description of the entrainment and transport process it is evident that the initial flow depth t_o should, in general, have no influence upon the rate of air discharge $\bar{q}_a$ at least not as long as the outer edge of the spreading air bubbles has not yet reached the lower surface of the jet at the control section S (Fig. 7.10). If, however, the spreading air bubbles do intersect the lower free surface upstream from this control section - either on the leading plate or on the free surface - then the air discharge may well be influenced by the water depth t_o. We can therefore distinguish, for a given set of parameters, a certain minimum water depth, above which the air entrainment process is independent of t_o, and below which t_o is of importance.

The air entrainment processes as described above hold true for intermediate values of the Froude number and are subject to limitations at both ends of the scale. The lower end of validity is given by either one of the two facts that for maintaining a flow pattern as described, the jet flow must be supercritical ($F > 1$), and the geometry must be such that the jet strikes the wall (which requires a minimum Froude number as a function of θ_o, a and α). If these conditions are met, a β-F-relation according to eq. 7.3 is seen to exist up to a certain maximum Froude number (corresponding to the limiting water depth t_o), beyond which the process becomes dependent upon the boundary scale, and finally there exists, as an absolute upper limit, the condition that β cannot increase beyond the value at which the flow becomes fully saturated. The results of Renner's experimental investigation are given in Figs. 7.11 through 7.14, in which the relative air discharge β is plotted as a function of the Froude number F for various boundary geometries. All diagrams have in common that β increases proportional to F^2 up to values of ($F = 9$) and with further increase of F begins to level off towards an asymptotic value given by the saturation limit. It can therefore be concluded that ($F = 9$) marks the limit from which on the depth of flow begins to have an influence upon the air discharge:

$$\text{for } F < 9 : \quad \beta = k F^2 \quad \text{or} \quad \frac{q_a}{V_o^3/g} = \text{const} \qquad (7.14)$$

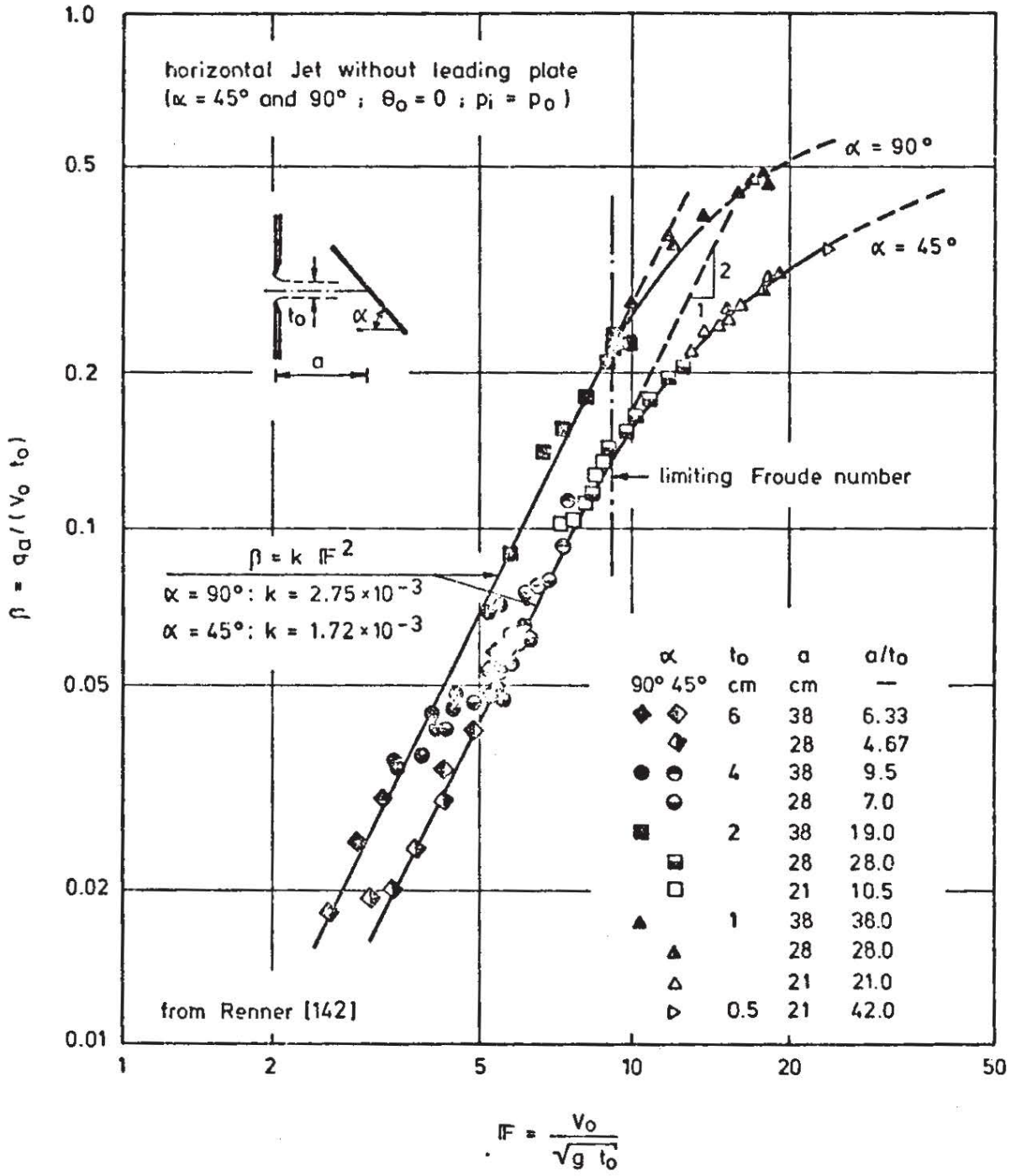

FIG. 7.11 RELATIVE AIR ENTRAINMENT IN A HORIZONTAL JET WITHOUT LEADING PLATE

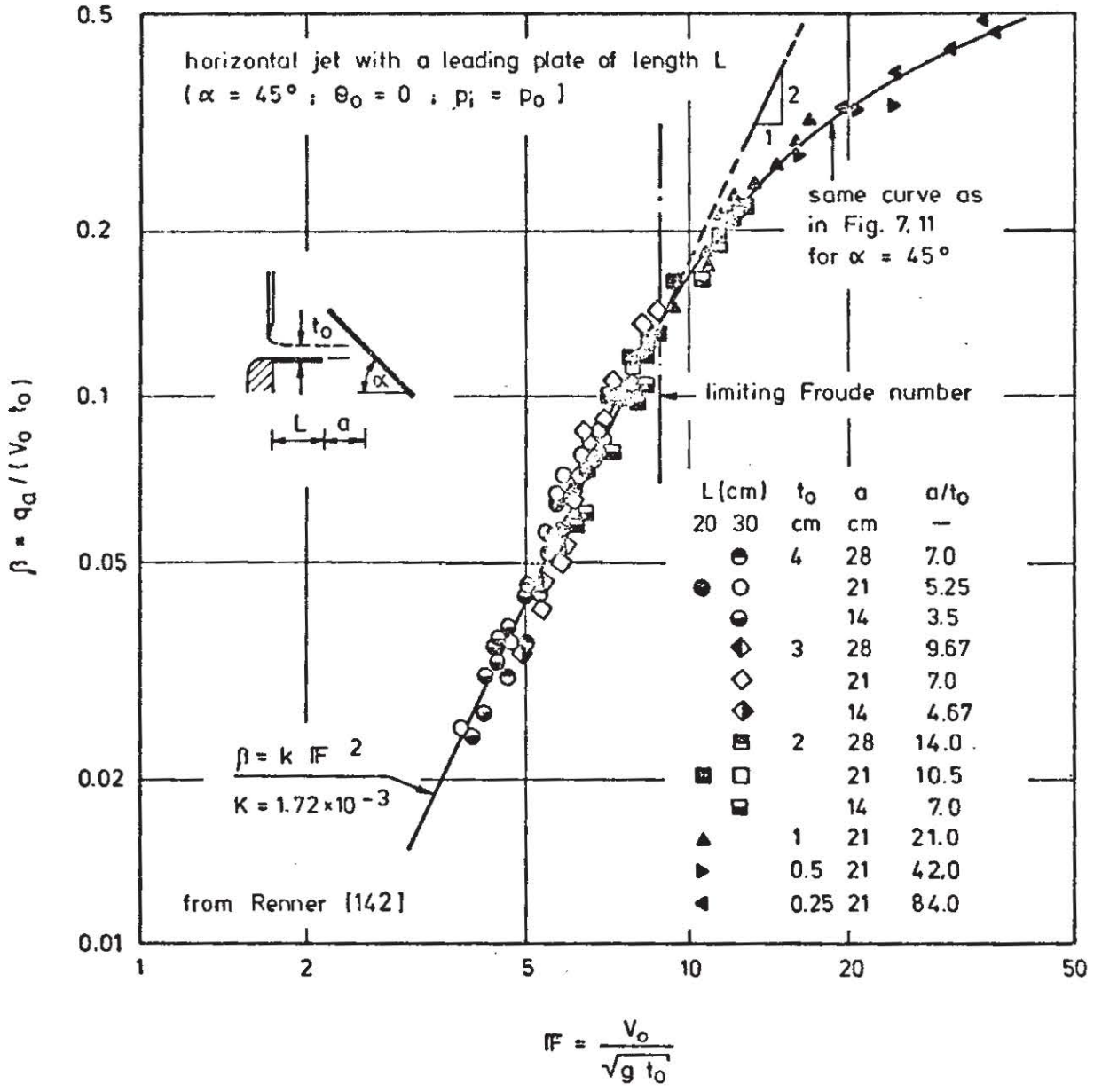

FIG. 7.12 RELATIVE AIR ENTRAINMENT IN A HORIZONTAL JET WITH LEADING PLATE

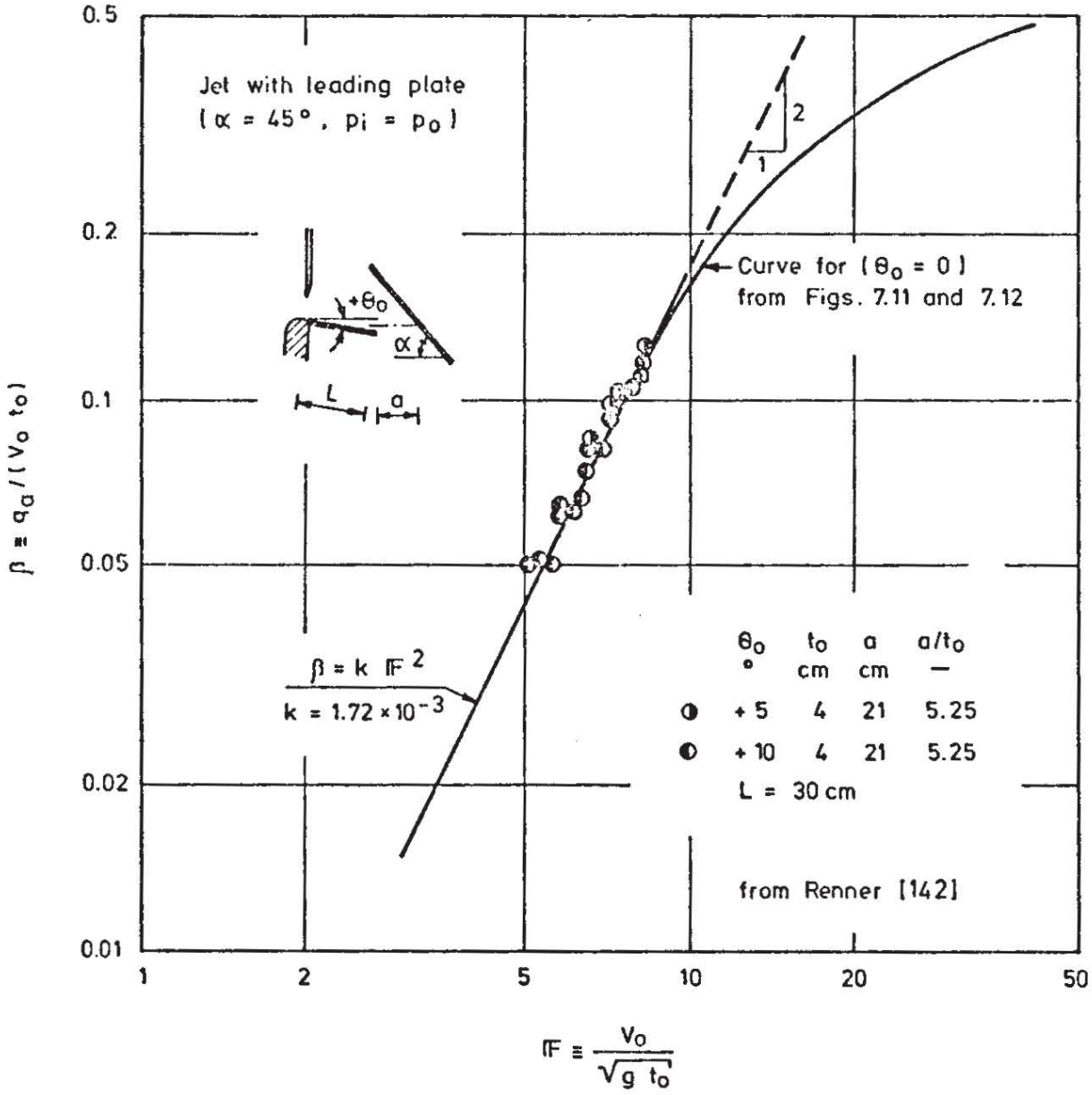

FIG. 7.13 VARIATION OF THE INITIAL ANGLE θ_o

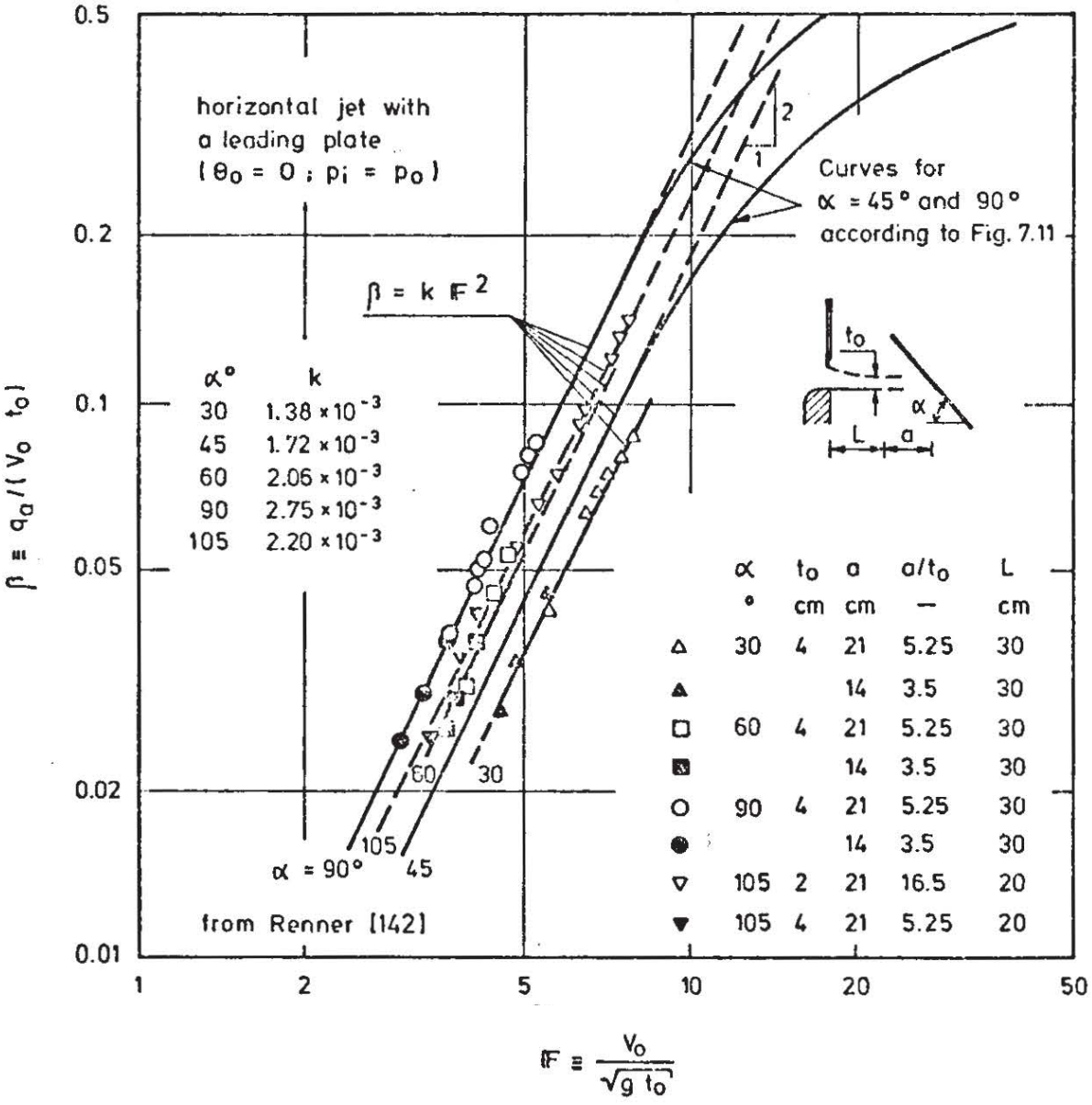

FIG. 7.14 RELATIVE AIR ENTRAINMENT β FOR VARIOUS WALL INCLINATIONS α

which indicates (see eq. 7.3) that the process is independent of the boundary length scale, and

$$\text{for } \mathbb{F} > 9: \quad \beta = f(\mathbb{F}, \text{geometry}); \quad \frac{q_a}{V_o^3/g} \neq \text{const} \qquad (7.15)$$

because of the influence of the water depth. The demarcation between the two types of flow is clearly visible from photographs which show that for ($\mathbb{F} > 9$) the air-water mixture reaches the lower free surface of the jet upstream from the control section S.

In accordance with eq. 7.13, the β - $\mathbb{F}$ - relation has been investigated for various values of (a/t_o), α and θ_o. Comparative tests with a leading plate of length L (Fig. 7.12) and without leading plate (Fig.7.11) show no influence of the leading plate within the range ($0 \leq L/t_o \leq 120$). Figs. 7.11 and 7.12 show furthermore clearly that for α = const and θ_o = const, the parameter a/t_o seems to have no influence upon the relationship within the limits investigated ($3.5 \leq a/t_o \leq 84$). From Fig. 7.13, it is evident that a slight inclination θ_o of the jet does not seem to affect the air discharge noticeably ($0 \leq \theta_o \leq +10^\circ$). Hence, relation 7.13 reduces to:

$$\beta = f(\mathbb{F}, \alpha) \quad \text{for} \quad \left\{ \begin{array}{rcl} 0 & \leq & L/t_o \leq 120 \\ 3.5 & \leq & a/t_o \leq 84 \\ 0 & \leq & \theta_o \leq +10^\circ \end{array} \right\} \qquad (7.16)$$

The influence of the plate inclination α upon the relationship is seen from Fig. 7.14, which shows that the relative air discharge attains maximum values for $\alpha = 90^\circ$ (vertical plate) and decreases both for larger and smaller inclination angles α . In Fig. 7.15, the relation

$$k \equiv \frac{q_a}{V_o^3/g} = f(\mathbb{F}, \alpha)$$

is plotted, which shows clearly the Froude-number ranges in which this ratio is a constant or varies with $\mathbb{F}$, respectively. The values of k (or $q_a/(v_o^3/g)$ for ($\mathbb{F} \leq 9$) are plotted in Fig. 7.16 as a function of α , which shows that the largest values of k occur at $\alpha = 90^\circ$.

If the relative air discharge for the jet impinging on a wall is compared to the relative air entrainment in a free hydraulic jump ($k_e = 5 \times 10^{-3}$) then the ratio of the respective k-values indicates that for a horizontal jet striking a vertical wall ($\alpha = 90^\circ$), about 55 % of the entrained air is actually transported out of the control section, whereas for ($\alpha = 30^\circ$) this percentage (a kind of "efficiency") drops to about 28 %, under the assumption that the amount of air entrained at the toe is always the same as in a free hydraulic jump.

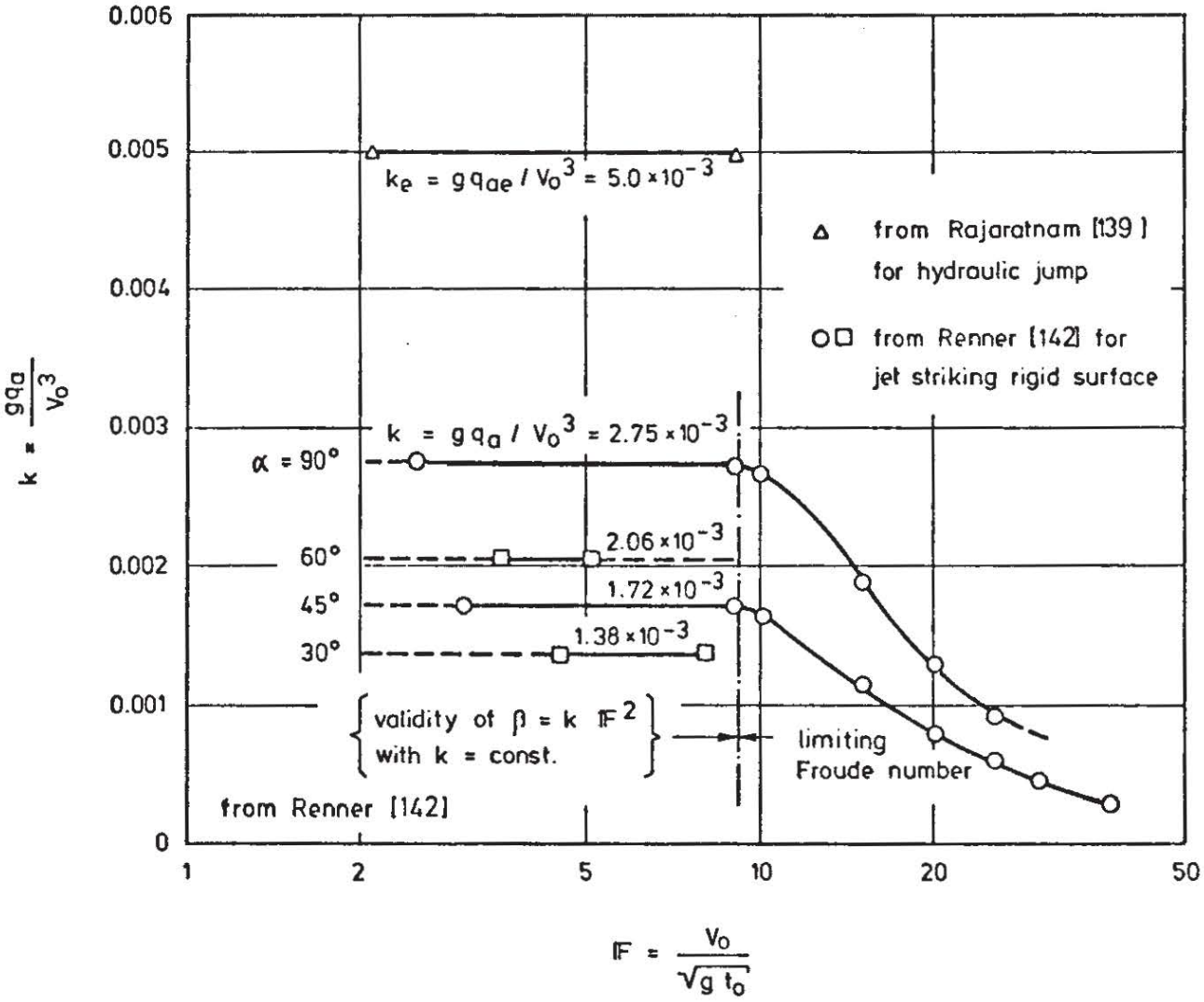

FIG. 7.15 DEPENDENCE OF THE FACTOR k UPON THE FROUDE NUMBER

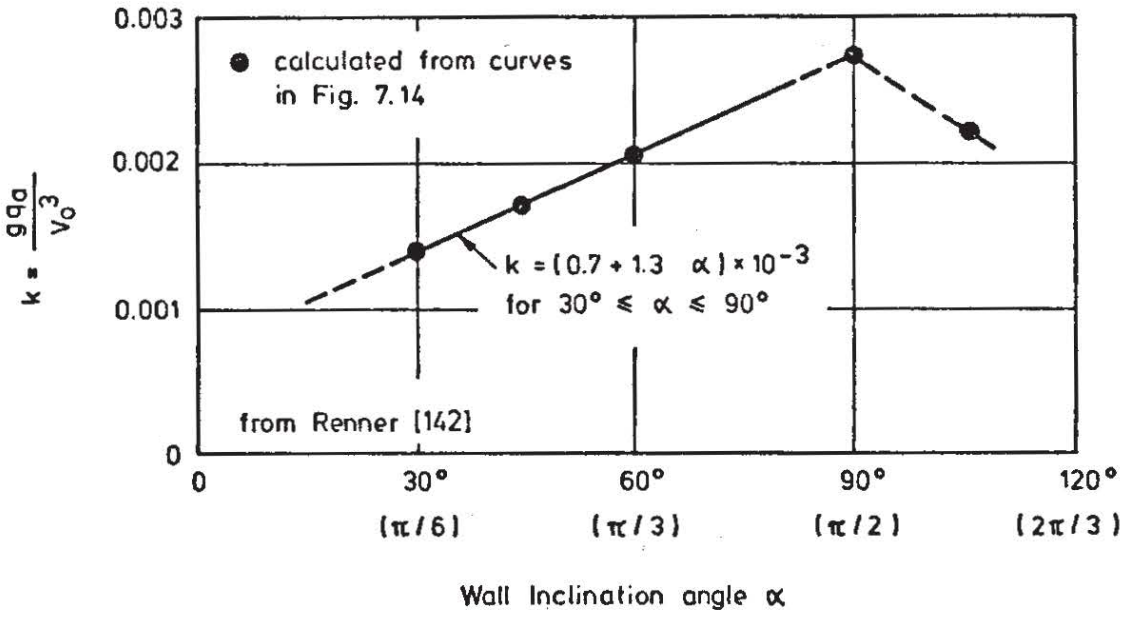

FIG. 7.16 DEPENDENCE OF k UPON THE WALL INCLINATION ANGLE FOR FROUDE NUMBERS SMALLER THAN THE LIMITING ($IF \leq 9$)

7.4 Air Entrainment of a Jet Penetrating a Liquid Surface

When a liquid jet penetrates a free liquid surface with sufficient velocity to give rise to intensive shearing forces, the air moving in the boundary layer of the jet will penetrate the free surface and thus produce an air-water mixture. For the case of a laminar circular vertical water jet penetrating a free water surface at rest, Lin [113] studied the conditions under which air entrainment begins to occur. According to this study, air entrainment inception is characterized by the relation (Fig. 7.17)

$$\mathrm{IR} = 0.045\ \mathrm{W}^{1.35} \qquad (7.17)$$

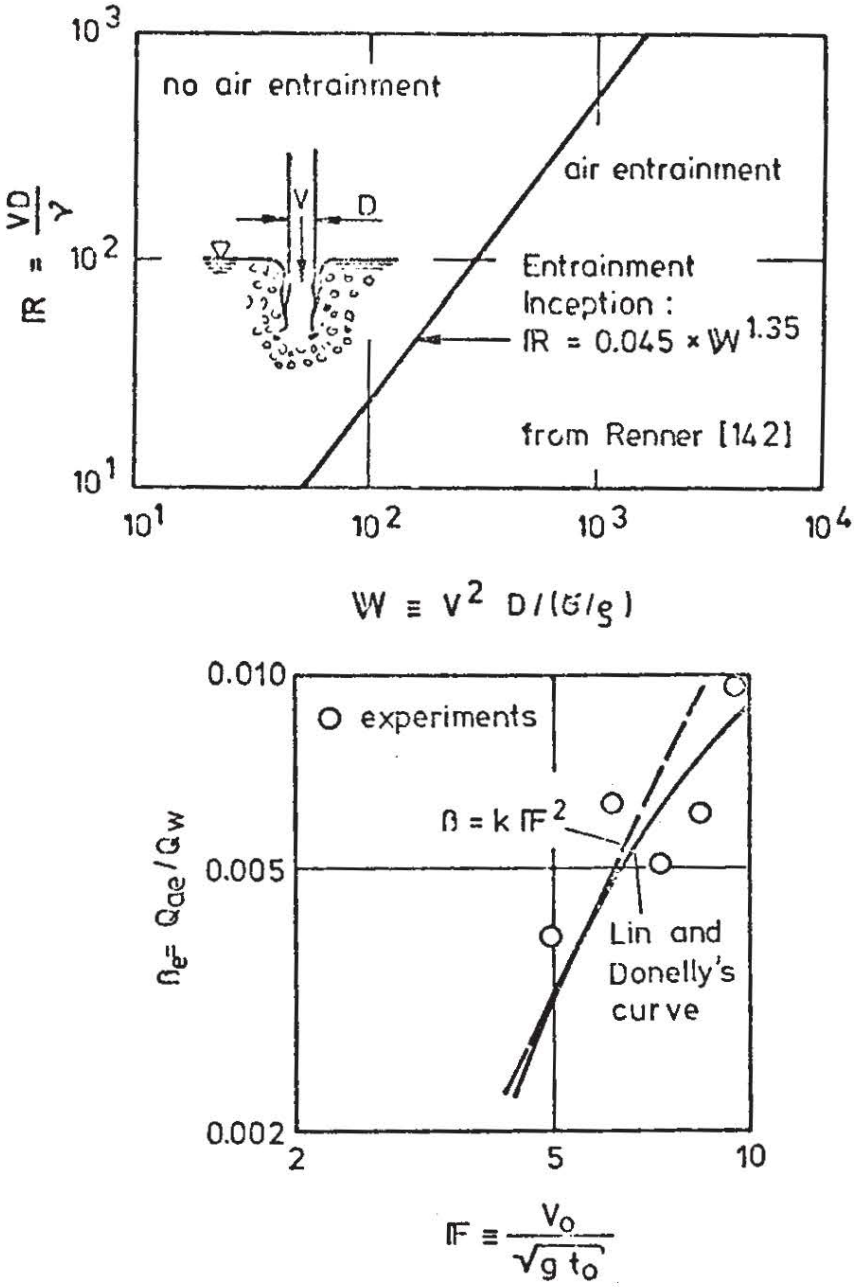

FIG. 7.17 CONDITIONS FOR ENTRAINMENT INCEPTION AND RELATIVE QUANTITY OF ENTRAINED AIR ACCORDING TO LIN AND DONELLY [113]

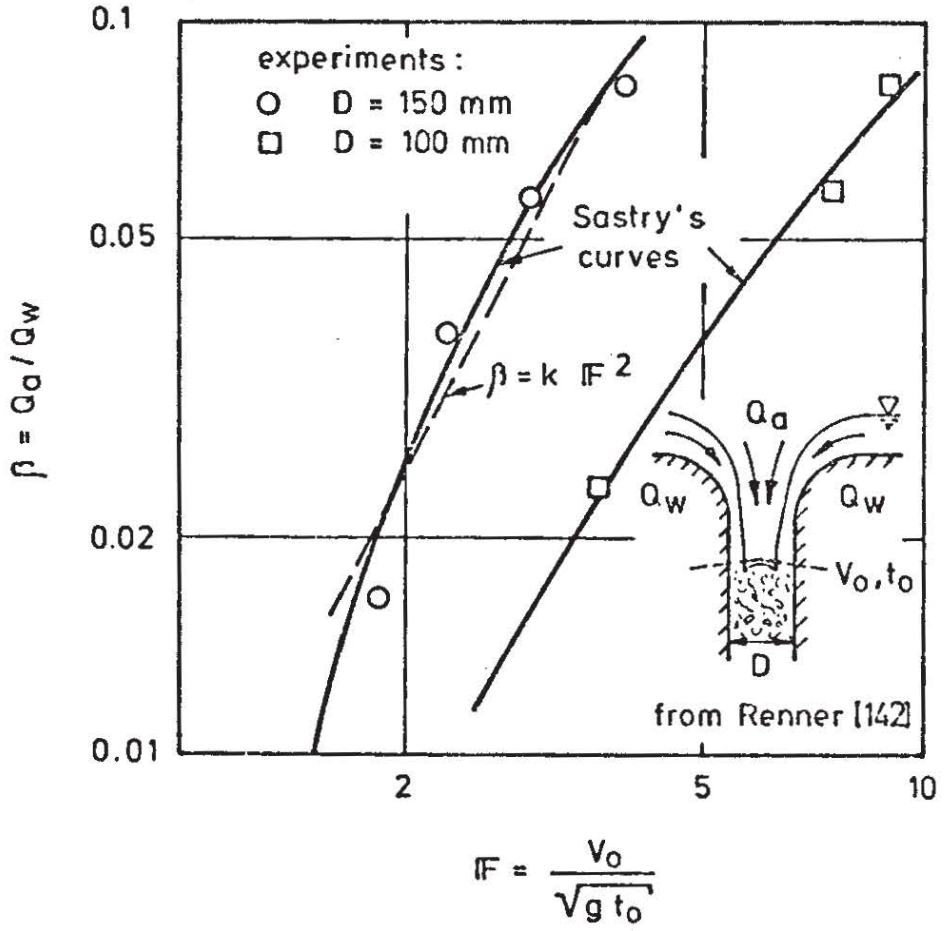

FIG. 7.18 AIR ENTRAINMENT IN A RINGSHAPED WALL JET ACCORDING TO SASTRY [151]

Lin only performed a few measurements of the quantity of air entrained per unit time, which show considerable scatter (Fig. 7.17), but nevertheless seem to support the existence of an entrainment relationship of the type

$$\beta_e = k_e \, F^2 \text{ with } \quad k_e \approx (0.1 \text{ to } 0.2)\ 10^{-3} \qquad (7.18)$$

Sastry [151] investigated the air entrainment of circular vertical drop structures, in which the downstream conditions are such that the vertical wall jet formed in the structure penetrates a free water surface (Fig. 7.18). He performed a small-scale hydraulic model study with two geometrically smilar models of different size. He also found a relationship of the type ($\beta = k\,IF^2$) for each model size - however, the observed values of k differ considerably for the two model sizes investigated. This discrepancy or "scale effect" is believed to be due to the fact that the transport conditions for the air-water mixture at the downstream end have not been modeled correctly: in a Froude model, they are necessarily scaled according to Froude's law, whereas the flow conditions and the transport capacity of the pipe flow depend upon the Reynolds number. The pipe flow Reynolds number was different in the two models, and at the small model scales used not yet large enough to ensure fully turbulent pipe flow conditions (and hence indepndence of the Reynolds number).

Wisner [191] studied the air entrainment due to two-dimensional flow of water over a sharp-crested, ventilated weir, which reattaches to an inclined surface on the downstream side and thereby forms a water pool between weir and nappe (Fig. 7.19). One peculiarity of this configuration is the fact that here the air entraining interface is located below the main flow. As long as there is no restriction to the air supply to the enclosed pocket, the experimental relation between ß and F given in Fig. 7.19 is found to exist. The experimental values in this case obviously do not support the ($\beta = k F^2$) relationship found in all other instances: the reason for the discrapancy is not evident at this time, nor is the observed trend very well documented by the experiments, since the Froude number only varied over a small range ($3.5 \leq F \leq 5$).

The related flow configuration of a vertical fluid jet penetrating a free surface from below has been studied by Higginbottom [71] . From his experimental results, Renner [142] deduced the relationship for air entrainment inception given in Fig. 7.20. No measurements of the entrained air quantities are available in this case.

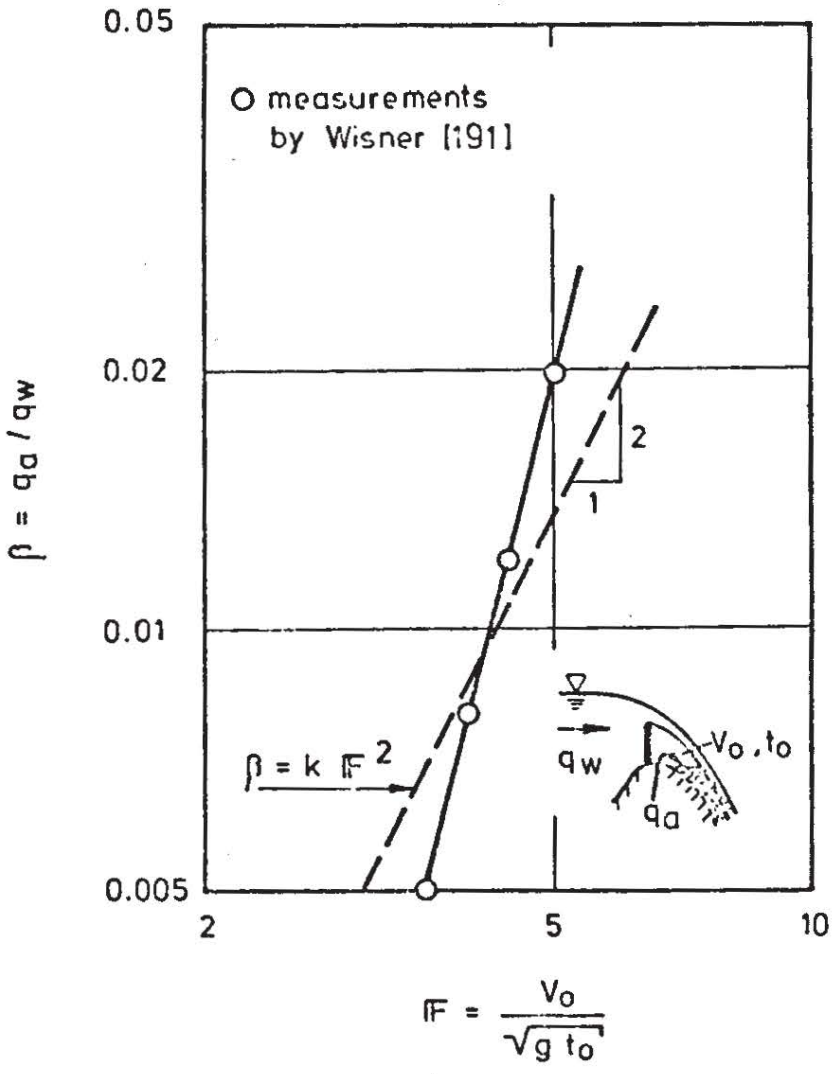

FIG. 7.19 AIR ENTRAINMENT BEHIND A SHARP-CRESTED WEIR

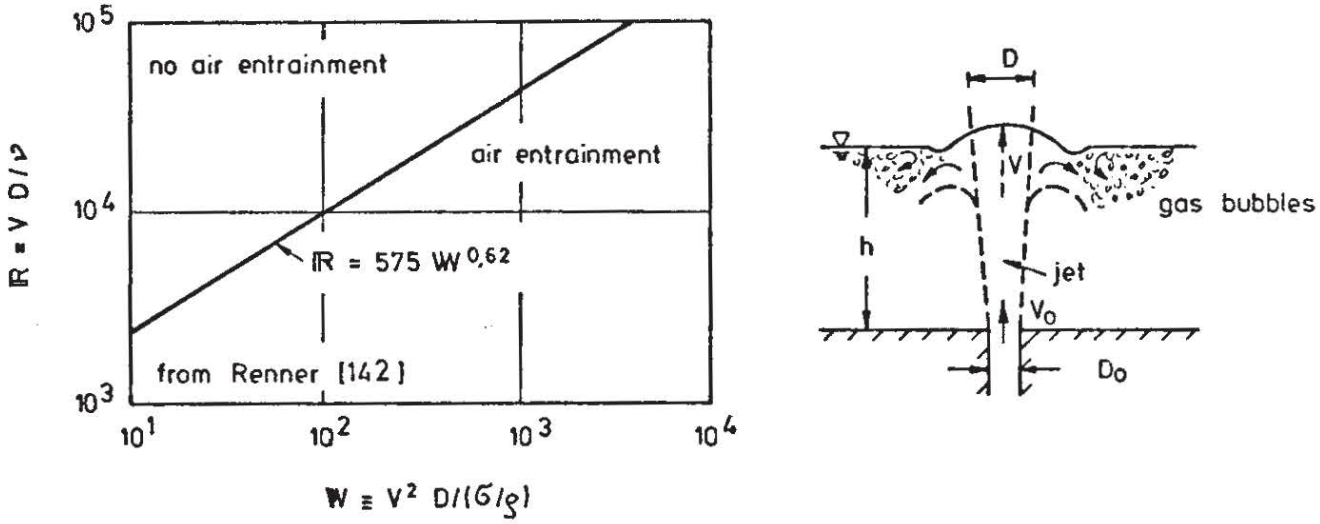

FIG. 7.20 AIR ENTRAINMENT INCEPTION AT A FREE SURFACE DISTURBED BY A VERTICAL JET FROM BELOW

7.5 Air Entrainment in Vortices and Breaking Waves

Air entrainment in vortices can be observed, for instance, on pump intakes, on vortex drop structures, or in the famous "bathtub vortex". According to Holtorff [78] , the air entrainment in a vortex is due to velocity fluctuations in the vortex, which cause the funnelshaped water surface above the vortex to fluctuate and thereby pinch off air pockets, which are transported away by the vortex flow. Air entrainment by vortices has been investigated by Holtorff [78] , Kleinschroth [93] and Quick [137] .

Air entrainment in breaking waves has been studied experimentally by Miller [121] . He was able to show by means of stroboscopic photography, that cylindrical air enclosures are formed in front of and parallel to the wave crest and that air is entrained into the water whenever these enclosures collapse. Führböter [47] investigated the significance of entrained air upon energy dissipation in breaker zones, without, however, touching upon the quantities of entrained air involved in the process.